

Room-temperature 1.5 μm photoluminescence of Er^{3+} -doped $\text{Al}_x\text{Ga}_{1-x}\text{As}$ native oxides

L. Kou,^{a)} D. C. Hall,^{b)} and H. Wu

Department of Electrical Engineering, University of Notre Dame, Notre Dame, Indiana 46556

(Received 13 March 1998; accepted for publication 24 April 1998)

Data are presented demonstrating 300 K, continuous wave (cw) photoluminescence near $\lambda = 1.53 \mu\text{m}$ from Er-implanted $\text{Al}_{0.8}\text{Ga}_{0.2}\text{As}$ films oxidized in water vapor ($\text{N}_2 + \text{H}_2\text{O}$, 500 °C) and annealed (1 h, 700 °C) in $\text{Ar} + \text{O}_2$. The 40 nm full width at half-maximum (FWHM) spectra are 1.5 \times broader and $\sim 10\times$ more intense relative to spectra from unoxidized but annealed samples. The fluorescence decay shows a $\tau = 7$ ms lifetime, with a faster $\tau = 1.9$ ms component characteristic of a cooperative upconversion mechanism. The data suggest that $\text{Al}_x\text{Ga}_{1-x}\text{As}$ native oxides may provide a suitable host for rare-earth optical activity. © 1998 American Institute of Physics. [S0003-6951(98)00226-5]

The rare-earth (RE) elements have long been explored as optically active dopants in numerous glass and crystal hosts. Er^{3+} receives particular attention due to the fortuitous coincidence of its 1.54 μm optical transitions with the minimum attenuation window of standard silica optical fibers. Following upon the successful development of erbium-doped fiber amplifiers for telecommunications, there has been considerable recent research towards similarly doping elemental and compound semiconductors with Er^{3+} and other rare earths.^{1,2} These efforts are motivated primarily by the promise of integrating optoelectronic functions into conventional Si microelectronics, but also by the potential for realizing a new class of wavelength-stable light emitters and amplifiers in III–V materials. At the same time, numerous researchers have been pursuing various other Er-doped thin film materials for the development of new planar waveguide integrated optoelectronics technologies.³ Compared to established oxide and fluoride insulator hosts, it has generally been found to be more difficult in semiconductors to incorporate RE dopants in an optically active (trivalently ionized) state. Also, direct electrical excitation processes in RE-doped semiconductors are not yet well understood and will perhaps be less efficient than conventional optical pumping schemes.

In this letter, we propose and demonstrate an approach for incorporating RE ions into Al-bearing III–V compound semiconductor systems by converting the RE-doped III–V crystal to its native oxide through the wet-thermal oxidation process discovered for AlGaAs in 1990 by Dallesasse *et al.*⁴ With this approach, the RE-doped native oxide regions could ultimately be optically excited by a monolithically integrated semiconductor pump laser. We present data demonstrating room temperature (300 K), continuous wave (cw) photoluminescence from Er^{3+} -doped AlGaAs native oxides. The native oxides of AlGaAs, formed by exposing a high-Al-composition $\text{Al}_x\text{Ga}_{1-x}\text{As}$ alloy film (typically $x \geq 0.5$) to water vapor ($\text{N}_2 + \text{H}_2\text{O}$) at an elevated temperature (400–550 °C), have been extensively employed in various optoelectronic and electronic device structures, most notably vertical-cavity surface-emitting lasers (VCSEL's).^{5,6} Identifi-

fied via electron diffraction patterns to be an amorphous solid solution of $(\text{Al}_x\text{Ga}_{1-x})_2\text{O}_3$,⁶ these native oxides are closely related to the Al_2O_3 films being explored by other researchers as a potential host for Er^{3+} .^{7,8} A low-loss compact Er-doped Al_2O_3 waveguide amplifier has recently been fabricated by sputter deposition followed by ion implantation.⁹ It has been suggested that the similarity in valency and lattice constants between Al_2O_3 and Er_2O_3 should allow the incorporation of high Er concentrations into Al_2O_3 films.⁷ For this reason, Al is also an effective codopant in silica glass fibers for enhancing Er incorporation and raising the concentration quenching limit.¹⁰

The starting material in our experiments is grown by molecular beam epitaxy (MBE) on a GaAs substrate and consists of a 1 μm $\text{Al}_{0.8}\text{Ga}_{0.2}\text{As}$ layer capped by $\sim 200 \text{ \AA}$ GaAs. The structures are doped after growth via ion implantation using doubly ionized Er as a source at an implant potential of 80 kV and using a dose of $1 \times 10^{15} \text{ cm}^{-2}$. Using the Monte Carlo program TRIM'95,¹¹ the Er^{3+} implantation profile is estimated to have a range of 460 \AA and a straggle of 180 \AA , with a peak concentration of about $2 \times 10^{20} \text{ cm}^{-3}$, and a maximum ion penetration depth of $\sim 1500 \text{ \AA}$. We note that Polman has reported that the TRIM program underestimates both the range and straggle of Er implantation profiles in Si by up to a factor of 2.³ After the GaAs cap layer is selectively removed using a citric acid/hydrogen peroxide etch, the samples are oxidized in a 2-in. tube furnace for 1 h at a temperature of 500 °C under a 0.66 l/min flow of N_2 bubbled through 95 °C deionized water. Full oxidation of the $\text{Al}_{0.8}\text{Ga}_{0.2}\text{As}$ material is verified by both a prism coupler measurement and a scanning electron microscope (SEM) cross-section measurement (data not shown). Postannealing is done open tube in an $\text{Ar} + \text{O}_2$ ambient at temperatures ranging from 600 to 900 °C, as discussed further below. For the purpose of comparing PL spectra, unoxidized Er-doped $\text{Al}_{0.8}\text{Ga}_{0.2}\text{As}$ films are also annealed under the same conditions, but with a 1000 \AA PECVD Si_3N_4 cap layer and in proximity to a GaAs wafer to protect against thermal decomposition.

PL measurements are performed at room temperature by exciting the Er^{3+} ions into their $^4\text{F}_{7/2}$ manifold using the 488 nm line of an Ar^+ ion laser. The cw pump beam is mechani-

^{a)}Electronic mail: lkou@nd.edu

^{b)}Electronic mail: dhall@nd.edu

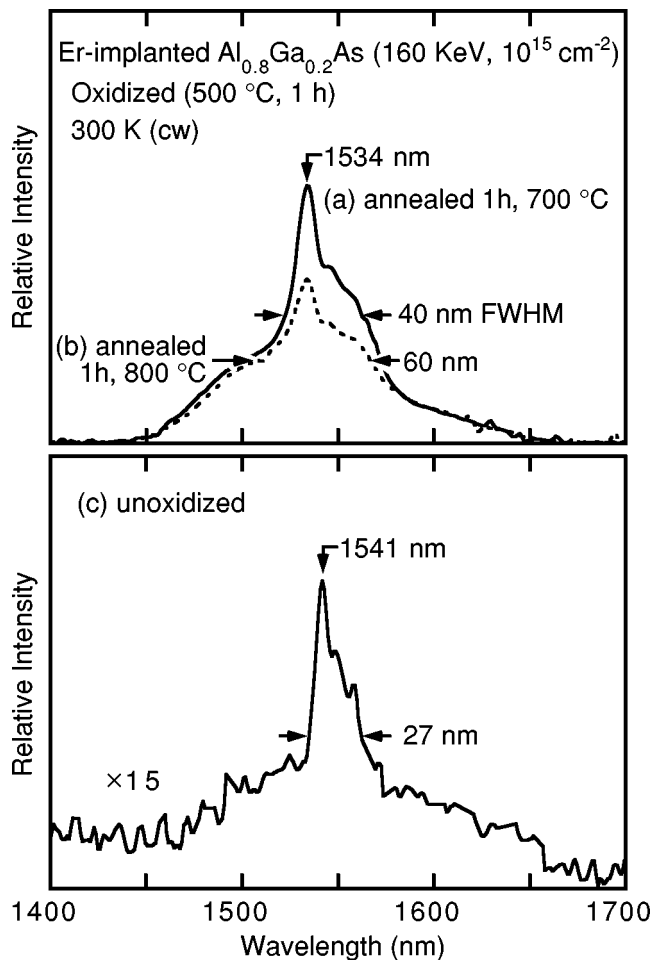


FIG. 1. Room-temperature PL spectra from Er implanted (10^{15} Er/cm 2 , 160 keV) $\text{Al}_{0.8}\text{Ga}_{0.2}\text{As}$ films (a) after oxidation (500 °C, 1 h) and annealing in Ar+O $_2$ (1 h, 700 °C), (b) after oxidation (500 °C, 1 h) and annealing in Ar+O $_2$ (1 h, 800 °C), and (c) unoxidized but annealed in N $_2$ (1 h, 700 °C). ($\lambda_{\text{pump}}=488$ nm, resolution ~ 1.7 nm).

cally chopped at 20 Hz. The luminescence is spectrally analyzed with a 0.5 m grating monochromator and detected with a Northcoast EO-817L liquid nitrogen-cooled Ge detector and lock-in amplifier. PL spectra for the Er-implanted $\text{Al}_{0.8}\text{Ga}_{0.2}\text{As}$ are shown in Fig. 1 for samples (a) oxidized (500 °C, 1 h) and annealed (1 h, 700 °C), (b) oxidized (500 °C, 1 h) and annealed (1 h, 800 °C), and (c) annealed (1 h, 700 °C) only (unoxidized). The amplitude scale of the weaker PL spectrum in Fig. 1(c) is magnified 15 times relative to Figs. 1(a) and 1(b). All spectra are excited with a pump power of 0.32 W focused to a ~ 250 μm diameter spot. The spectral resolution is ~ 1.7 nm. Comparison reveals Er $^{3+}$ PL spectra which are quite different for the native oxide and unoxidized semiconductor hosts. For Er $^{3+}$ ions in the native oxide, the central peak is 1.534 μm and the FWHM are (a) 40 nm and (b) 60 nm, typical of $^4\text{I}_{13/2} \rightarrow ^4\text{I}_{15/2}$ Er $^{3+}$ transitions in Al_2O_3 . 7,8 For Er $^{3+}$ ions in the $\text{Al}_{0.8}\text{Ga}_{0.2}\text{As}$ semiconductor host, the central peak is 1.541 μm and the FWHM is 27 nm.

PL excitation spectra measured at different Ar $^+$ ion laser lines also indicate a difference in excitation mechanisms between the oxide and semiconductor hosts while confirming that the Er $^{3+}$ ions in the oxide host are resonantly pumped to their $^4\text{F}_{7/2}$ manifold. For an excitation power of 0.25 W, the

oxide sample of Fig. 1(a) yields relative intensities (in parentheses) of the 1.534 μm PL peak at the different pump wavelengths of: 457.9 nm (0.13), 472.7 (0.03), 476.5 (0.04), 488.0 (1.00), 496.5 (0.20), 501.7 (0.13), and 514.5 (0.44). For the unoxidized sample of Fig. 1(c), the relative peak PL intensities are invariant with excitation wavelength within $\pm 1\%$, indicating that band-to-band absorption by the semiconductor host likely plays an intermediate role in the Er $^{3+}$ excitation process. Defects not removed by annealing may also contribute to a broadened absorption spectra.

The PL peak intensity of Er $^{3+}$ in the oxide host after annealing at 700 °C [Fig. 1(a)] increases by a factor of more than 20 compared to an unannealed sample oxidized at the same time. For the latter, the quality of the weak PL spectrum (not shown) is too poor for quantitative comparison. Annealing at higher temperatures than 700 °C leads to a decrease in the PL intensity and degradation of the oxide film. Polman has reported that the optimum annealing temperatures for both soda-lime silicate glass and pure silica lie just below transformation temperatures. 3 Thus, a possible cause of the PL intensity decrease we observe between (a) 700 °C and (b) 800 °C anneals is a phase transformation which occurs for amorphous $(\text{Al}_{0.8}\text{Ga}_{0.2})_2\text{O}_3$ somewhat above 700 °C. 12 Amorphous Al_2O_3 undergoes a similar transformation to $\gamma\text{-Al}_2\text{O}_3$ at ~ 800 °C. 13 A comparable ~ 55 nm FWHM spectral width has been reported for Er-implanted Al_2O_3 deposited with a cubic polycrystalline structure. 3 Further studies are required to accurately determine the structure and phase transformation temperature of the oxides in this work. A second possible cause of the observed degradation of oxide quality and PL intensity is thermal decomposition of the underlying GaAs substrate due to the overly aggressive open-tube annealing conditions. Significant oxide surface roughening PL intensity degradation is noticed for anneals done at 900 °C.

Annealing of RE-doped materials is routinely carried out to enhance the optical activation of dopants, and to heal irradiation damage in ion-implanted materials. As the semiconductor crystal is altered in structure and composition upon oxidation, we did not attempt to recrystallize the films through annealing previously. In our experiments, the increase in PL intensity upon annealing in an Ar+O $_2$ atmosphere is attributed primarily to a reduction in the concentration of luminescence-quenching OH $^-$ (hydroxyl) compounds in the oxide. Because our oxidation process requires water vapor, the oxidized layers retain OH $^-$ groups. The formation of Al-O-H compounds in AIAs native oxides has been observed with SIMS analysis. 14 Such hydroxyl compounds are well-known luminescence quenching centers in other Er-doped glasses. $^{3,15-17}$ Annealing in Ar has been shown to be effective in reducing hydroxyl groups in GeS $_2$ glass 15 and alumino-silicate glasses formed by the sol-gel process. 16,17 The PL intensity of oxidized samples annealed in pure N $_2$ (data not shown) is significantly weaker than that of Fig. 1(a), indicating that reduction of OH $^-$ is the primary role of the anneal in Ar+O $_2$. Other oxidized samples annealed in Ar alone have a comparable PL intensity, indicating that the addition of O $_2$ may be unnecessary.

Fluorescence decay measurements are performed to determine the kinetics and lifetime of the Er $^{3+}$ first excited

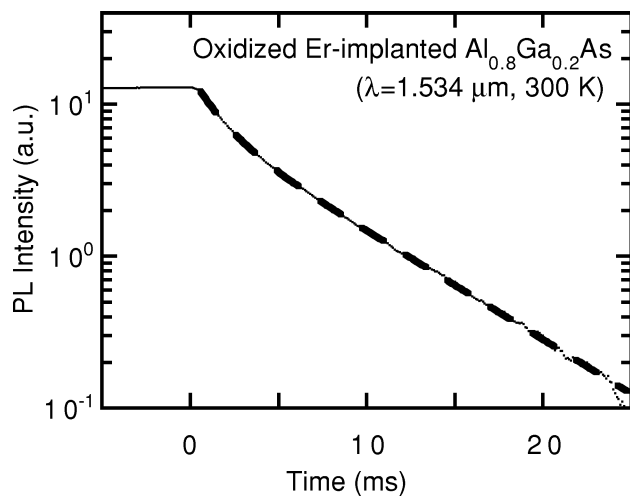


FIG. 2. Fluorescence decay curves for the Er-implanted native oxide PL spectra of Fig. 1(a), measured at $\lambda = 1.534 \mu\text{m}$ after switching off the 488 nm pump source at $t = 0$ ms. The dashed line shows a double-exponential fit with lifetimes $\tau_1 \approx 7$ ms and $\tau_2 \approx 1.9$ ms, with the initial fast decay component characteristic of cooperative upconversion.

state ($^4I_{13/2}$). From steady-state excitation, the pump source is mechanically switched off with a chopper wheel (cutoff time ~ 0.22 ms) and the fluorescence decay is monitored using a faster but less sensitive thermoelectrically cooled InGaAs detector having a rise time of ≤ 0.2 ms. The decay curves are averaged on a digitizing oscilloscope. Figure 2 shows the fluorescence decay of the $\lambda = 1.534 \mu\text{m}$ spectral peak for the Er-implanted native oxide PL data of Fig. 1(a). The relative intensity data are plotted on a logarithmic scale. The nonexponential decay is well described by a double-exponential curve fit (correlation coefficient $r = 0.99998$), as shown by the thicker, dashed line. The decaying PL intensity I_{PL} is proportional to the total density Er_{act} of active Er ions

$$I_{\text{PL}} \propto (\text{Er}_{\text{act}}) = (\text{Er}_i) \exp(-t/\tau_1) + (\text{Er}_c) \exp(-t/\tau_2), \quad (1)$$

where $[\text{Er}_i]$ and $[\text{Er}_c]$ are two distinct types of optically active Er ions having lifetimes $\tau_1 \approx 7$ ms and $\tau_2 \approx 1.9$ ms, respectively. The slower decay is attributed to (Er_i) isolated Er^{3+} ions. The fast decay component is characteristic of a cooperative upconversion mechanism¹⁸ associated with $[\text{Er}_c]$ ions where a transfer of energy occurs between two interacting ions in the excited state, promoting the acceptor ion to a higher energy level and nonradiatively quenching the donor ion back down to the ground state. From our fit using Eq. (1), the distribution of active ions among these two types is approximately equal. The $\sim 2 \times 10^{20} \text{ cm}^{-3}$ peak Er concentration in our unoxidized samples corresponds to a moderate 0.4 at. % Er after oxidation. Our data are consistent with the observation of cooperative upconversion in Er-implanted Al_2O_3 waveguides as the dominant deexcitation mechanism at “high” (1.4 at. %) concentrations, and greatly reduced but still present at “low” (0.12 at. %) Er concentrations.¹⁸ Through the use of a more uniform and lower concentration level, as achievable via multiple-high-energy implants,¹⁸ upconversion effects should be substantially reduced. The

weaker PL intensities for the other samples in our study (the unoxidized but annealed semiconductor and the unannealed oxide) prevent an accurate fluorescence decay measurement. As a possible alternative to ion implantation, the rare-earth dopants could also be incorporated through direct doping of the semiconductor material during crystal growth, as has been demonstrated with MBE-grown AlGaAs.¹⁹

In conclusion, the native oxide of Er-implanted $\text{Al}_{0.8}\text{Ga}_{0.2}\text{As}$ shows strong room temperature, cw photoluminescence at $1.533 \mu\text{m}$. Postannealing in Ar+O₂ greatly increases the PL intensity and lifetime, which we attribute to the reduction of the OH content in the oxide. Further studies are required to determine if these probable luminescence-quenching OH compounds can be adequately eliminated following oxidation, and whether sufficiently high Er concentrations can be achieved for adequate emission cross sections without upconversion effects. With further process optimization, such native oxides of Al-bearing III–V compound semiconductor alloys may prove to be a suitable host for optical activity of various rare-earth dopants.

The authors would like to thank Dr. J. K. Furdyna for MBE material growth materials and Dr. Y. Zhou for helpful information on gas-ambient annealing. This work was supported by NSF CAREER Award No. ECS-9502705.

- ¹G. S. Pomrenke, P. B. Klein, and D. W. Langer, *Mater. Res. Soc. Symp. Proc.* **301** (1993).
- ²S. Coffa, A. Polman, and R. N. Schwartz, *Mater. Res. Soc. Symp. Proc.* **422** (1996).
- ³A. Polman, *J. Appl. Phys.* **82**, 1 (1997).
- ⁴J. M. Dallesasse, N. Holonyak, Jr., A. R. Sugg, T. A. Richard, and N. El-Zein, *Appl. Phys. Lett.* **57**, 2844 (1990).
- ⁵D. G. Deppe, D. L. Huffaker, T. Oh, H. Deng, and Q. Deng, *IEEE J. Sel. Top. Quantum Electron.* **3**, 893 (1997).
- ⁶K. D. Choquette, K. M. Geib, C. I. H. Ashby, R. D. Twisten, O. Blum, H. Q. Hou, D. M. Follstaedt, B. E. Hammons, D. Mathes, and R. Hull, *IEEE J. Sel. Top. Quantum Electron.* **3**, 916 (1997).
- ⁷G. N. van den Hoven, E. Snoeks, A. Polman, J. W. M. van Uffelen, Y. S. Oei, and M. K. Smit, *Appl. Phys. Lett.* **62**, 3065 (1993).
- ⁸R. Serna and C. N. Afonso, *Appl. Phys. Lett.* **69**, 1541 (1996).
- ⁹G. N. van den Hoven, R. J. I. M. Koper, A. Polman, C. van Dam, J. W. M. van Uffelen, and M. K. Smit, *Appl. Phys. Lett.* **68**, 1886 (1996).
- ¹⁰W. J. Miniscalco, *J. Lightwave Technol.* **9**, 234 (1991).
- ¹¹J. F. Ziegler, J. P. Biersack, and U. Littmark, *The Stopping and Range of Ions in Solids* (Pergamon, New York, 1985).
- ¹²E. M. Levin, C. R. Robbins, and H. F. McMurdie, *Phase Diagrams for Ceramists* (American Ceramic Society, Columbus, OH, 1964), Figs. 310 and 2008.
- ¹³R. D. Twisten, D. M. Follstaedt, K. D. Choquette, and J. R. P. Schneider, *Appl. Phys. Lett.* **69**, 19 (1996).
- ¹⁴A. R. Sugg, N. Holonyak, Jr., J. E. Baker, F. A. Kish, and J. M. Dallesasse, *Appl. Phys. Lett.* **58**, 1199 (1991).
- ¹⁵A. J. Faber, D. R. Simons, Y. Yan, and H. de Waal, *Proc. SPIE* **2290**, 80 (1994).
- ¹⁶Y. Zhou, Y. L. Lam, S. S. Wang, H. L. Liu, C. H. Kam, and Y. C. Chan, *Appl. Phys. Lett.* **71**, 587 (1997).
- ¹⁷M. Benatsou, B. Capoen, M. Bouazaoui, W. Tchana, and J. P. Vilcot, *Appl. Phys. Lett.* **71**, 428 (1997).
- ¹⁸G. N. van den Hoven, E. Snoeks, A. Polman, C. van Dam, J. W. M. van Uffelen, and M. K. Smit, *J. Appl. Phys.* **79**, 1258 (1996).
- ¹⁹T. Zhang, J. Sun, N. V. Edwards, D. E. Moxey, R. M. Kolbas, and P. J. Caldwell, *Mater. Res. Soc. Symp. Proc.* **301**, 257 (1993).